Spectral Efficiency Optimization with Distributed Beamforming in UWB Based Implant Body Area Networks

Jie Ding
WiMed Research Centre
Department of Engineering
Macquarie University, Australia
Jie.Ding1@mq.edu.au

Eryk Dutkiewicz
WiMed Research Centre
Department of Engineering
Macquarie University, Australia
Eryk.Dutkiewicz@mq.edu.au

Xiaojing Huang
Computational Informatics
CSIRO
Sydney, Australia
Xiaojing.Huang@csiro.au

Gengfa Fang
WiMed Research Centre
Department of Engineering
Macquarie University, Australia
Gengfa.Fang@mq.edu.au

ABSTRACT

In this paper, a distributed beamforming problem is investigated based on spectral efficiency (SE) optimization for ultra-wideband (UWB) based implant body area networks (IBANs). We consider a relay network consisting of one implant source, several wearable relays, and one body network coordinator under the assumption that the individual relay power is constrained due to the Federal Communications Commission (FCC) regulations for UWB signals. Taking into account realistic wireless channels and relay locations, the SE optimization problem is mathematically formulated and solved by using convex optimization. Simulation results show that the proposed beamforming scheme is superior to other transmission schemes. Moreover, our numerical examples reveal that the relay location has a significant impact on the beamforming performance and the proposed beamforming scheme provides an efficient way to prolong the lifetime of the implant node.

Categories and Subject Descriptors

H.4 [**Information Systems Applications**]: Miscellaneous; D.2.8 [**Software Engineering**]: Metrics—*performance measures*

General Terms

Theory

Keywords

Spectral efficiency, distributed beamforming, UWB, implant body area networks

BODYNETS 2014, September 29-October 01, London, Great Britain

DOI 10.4108/icst.bodynets.2014.257010

1. INTRODUCTION

Wireless body area network (BAN) is an enabling technology for pervasive healthcare by using several sensors on/in the human body [1, 2]. Ultra-wideband (UWB) technology has a great potential for applications in BANs, owing to its simple electronics and low power consumption. In UWB based implant BANs (IBANs), the achievable data rate of direct transmission is often unsatisfactory because of the propagation blockage from the body torso as well as the low transmit power. Thus, spectral efficiency (SE), as a performance criterion related to the data rate, is one of the most critical concerns for UWB based IBANs. On the other hand, cooperative communication techniques have gained much attention in wireless networks which can achieve cooperative diversity gain that improves link reliability and SE [3].

Considerable research into cooperative transmission strategies has been conducted in wireless sensor networks (WSNs) regarding the SE [4, 5, 6, 7]. In [4], a single relay selection scheme was proposed to achieve the maximum SE and minimum outage probability. For multiple relay cooperation with perfect channel state information (CSI), distributed beamforming strategies have been developed to maximize SE subject to different power constrains under flat fading channels [5, 6]. In [7], the techniques of [5, 6] have been extended to the frequency selective fading channel scenarios. While aforementioned work mainly focused on the narrowband cases, it is not straightforward to apply them to the impulse-based UWB cases due to the special properties of UWB signaling such as analog transmission and dense resolvable multipath. Thus, some extensions of cooperative transmission strategies to UWB systems have been proposed in literature [8, 9, 10, 11]. However, the problem of distributed beamforming regarding SE for UWB based BANs is still an open issue.

Unlike conventional networks, BANs have many unique properties, e.g., distinct channel characteristics and very small network size, where the signal strength is mostly affected by the physical location of the nodes in relation to each other as well as the human body. Therefore for relay based cooperative BANs, the impact of relay location and channel path loss between nodes must be taken into account. In particular, both "in-body to on-body" and "on-body to on-body" channels are involved in cooperative IBANs, which makes the relay location a critical issue on the system performance. Thus, it is important to analyze the performance of distributed beamforming and evaluate the effect of relay location in UWB based IBANs.

In this paper, the SE optimization based distributed beamforming problem is investigated for UWB based IBANs. Explicitly, an IBAN consists of one implanted transmitter, several parallel wearable relays, and one body network coordinator. At coordinator and at each relay, a Rake receiver and matched filter are employed to capture the multipath energy, respectively. With this configuration, the proposed network beamforming is equivalent to a distributed power allocation, where each relay properly adjusts its own power such that the system SE can be maximized. Under the assumption that individual relay power is constrained due to the Federal Communications Commission (FCC) regulations for UWB signals, the network beamforming problem can be reduced to a quasiconvex optimization problem, which can be solved by using convex optimization. Simulation results show that the proposed beamforming scheme outperforms other transmission schemes. Moreover, the relay location plays an important role on the beamforming performance and our numerical examples reveal that the optimal relay location varies with the battery power limit of the implant node. Furthermore, given a targeted SE, the power consumption of the implant node is less as a larger the number of relays and the rake fingers at the coordinator are employed, which indicates the proposed beamforming scheme provides an efficient way to prolong the lifetime of the implant node.

The remainder of this paper is organized as follows. In Section II, the system and channel models are described. In Section III, the distributed beamforming transmission is introduced. In Section IV, the SE maximization for distributed beamforming is detailed. Simulation results are presented in Section V and the paper is concluded in Section VI.

2. SYSTEM AND CHANNEL MODELS

2.1 System Scenarios

Since two-hop cooperative communication is specified as an optional scheme in the IEEE 802.15.6 standard [1], the two-hop cooperative communication is considered in this paper. As shown in Fig. 1, a cooperative model for IBANs is proposed, where the transmitter node S (Source) is implanted in the human chest, and m wearable relay nodes (R_i, for i=1,...,m) and a body network coordinator D (Destination) are assumed to be on the same side of body surface. We denote the distance from S to D and penetration depth from S to the body surface by d_{SD} and d_r, respectively. On the body surface, we construct a xy-plane to present coordinates of m relays, where P is the projection of S on the body surface and it is set to be the origin point, and the x-axis is along P to D. In this paper, a special parallel relay topology is considered, where m relays have the same x-coordinate x_0 [mm] ($x_0 \geq 0$) and are evenly distributed along y-axis. With a given y-coordinate y_i [mm] for relay i, we have

$$d_{SR_i} = \sqrt{x_0^2 + y_i^2 + d_r^2},$$

and

$$d_{R_iD} = \sqrt{(x_0 - d_{SD}\sin\theta)^2 + y_i^2},$$

where d_{SR_i} and d_{R_iD} are the distances from S to relay i and relay i to D, respectively. $\theta = \arccos(d_r/d_{sd})$. It is worth to note that we herein study a two-step amplify-and-forward (AF) protocol. In the first step, S broadcasts its signal to relays, and during the second step, relays forwards their received signals to D.

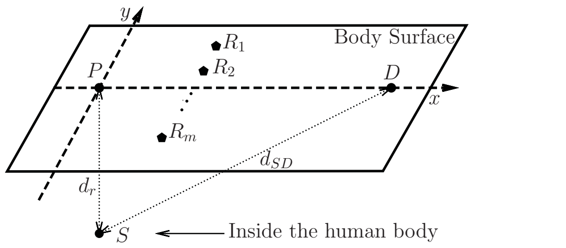

Figure 1: Proposed cooperative model for IBANs.

2.2 Channel Models

For cooperative transmission, two types of channel models need to be considered in UWB based IBANs, namely an "along-torso" channel model from relays to D and an "in-body" channel model from S to relays. Table 1 summarizes the path loss models with the corresponding parameters [12, 13].

Table 1: UWB based BAN Path Loss Models

"along-torso" channel	$PL_0^{dB}(d) = P_0 + 10n_0\log_{10}(\frac{d}{d_{r0}})$
P_0 [dB]	44.6
n_0	3.1
$d_{r0}[m]$	0.1
"in-body" channel	$PL_1^{dB}(d) = P_1 + a(d/d_{r1})^{n_1} + H$
P_1 [dB]	10
a	0.987
n_1	0.85
$d_{r1}[m]$	0.001

[1] P_i is the path loss at the reference distance, for i=0,1.
[2] d_{ri} is the reference distance, for i=0,1.
[3] n_i is the path loss exponent, for i=0,1.
[4] a is a fitting constant.
[5] H is a Gaussian distributed random variable with zero mean and standard deviation 7.84.

From the path loss models defined in the log scale, we can obtain the path losses in the linear scale from S to R_i and R_i to D as,

$$PL_{SR_i}(d_{SR_i}) = 10^{PL_1^{dB}(d_{SR_i})/10}, \quad i = 1, ..., m$$

and

$$PL_{R_iD}(d_{R_iD}) = 10^{PL_0^{dB}(d_{R_iD})/10}, \quad i = 1, ..., m$$

respectively.

For all the links considered, the energy-normalized channel impulse response (CIR) can be written as

$$h_k(t) = \sum_{l=0}^{L_k-1} \alpha_{l,k}\delta(t-\tau_{l,k}),$$

where $k \in \{SR_i, R_iD\}$ denotes the links from S to R_i and R_i to D respectively. L_k is the number of multipaths, $\tau_{l,k}$ is the delay of the lth path, and $\alpha_{l,k}$ is the gain of the lth path. Since real signals are employed in UWB systems, we are only interested in the real part of each path gain. Further detail on the delay profile for "along-torso" and "in-body" links can be found in [12] and [13], respectively.

3. DISTRIBUTED BEAMFORMING TRANSMISSION

For analytical simplicity, we present the IR-UWB signal model with pulse-amplitude modulation (PAM). The random time hopping (TH) or direct spread (DS) codes are not considered in this paper.

At S, every transmitted PAM symbol duration T_s consists of N_f consecutive frames each with duration T_f, where $T_s = N_f T_f$. The symbol information is conveyed by an ultrashort pulse waveform in each frame. Thus the transmitted symbol waveform can be expressed as

$$s(t) = b\sqrt{P_s}\sum_{j=0}^{N_f-1}\omega(t-jT_f), \; b = \pm 1 \tag{1}$$

where b is the transmitted symbol and P_s is the transmit power of the implant node and the value of P_s depends on the battery power limit of the implant node. $\omega(t)$ denotes the ultrashort pulse waveform with T_w duration, which has the unit energy $\int_{t=0}^{T_f}\omega^2(t) = 1$.

For all the links, it is assumed that channel $h_k(t)$ remains invariant over a symbol duration, but it changes from symbol to symbol. Thus, the received signal at relay i is given by

$$\begin{aligned} r_{SR_i}(t) =& b\sqrt{\frac{P_s}{PL_{SR_i}(d_{SR_i})}}\sum_{j=0}^{N_f-1} g_{SR_i}(t-jT_f) \\ &+ n_{SR_i}(t), \end{aligned} \tag{2}$$

where

$$g_{SR_i}(t) = \omega(t) * h_{SR_i}(t) = \sum_{l=0}^{L_{SR_i}-1}\alpha_{l,SR_i}\omega(t-\tau_{l,SR_i}), \tag{3}$$

and $n_{SR_i}(t)$ is the additive white Gaussian noise (AWGN) with zero mean and variance σ^2. $*$ represents convolution. T_f is set to be large enough to avoid the inter-symbol interference (ISI).

At each relay, a received pulse waveform matched filter is employed. During each frame duration, the output of the matched filter at relay i is given by

$$\begin{aligned} \bar{r}_{SR_i}(j) &= \int_{jT_f}^{(j+1)T_f} r_{SR_i}(t) g_{SR_i}(t-jT_f)dt \\ &= b\sqrt{\frac{P_s}{PL_{SR_i}(d_{SR_i})}}\xi_{T_f}(h_{SR_i}) + \bar{n}_{SR_i}(j), \end{aligned} \tag{4}$$

where $j \in [0, N_f-1]$. $\xi_{T_f}(h_{SR_i})$ is the captured multipath energy during T_f at relay i and $\bar{n}_{SR_i}(j)$ is still a white Gaussian noise with zero mean and variance $\xi_{T_f}(h_{SR_i})\sigma^2$.

After summing up all the outputs over N_f frames, the decision statistic b at relay i can be written as

$$b_{R_i} = bN_f\sqrt{\frac{P_s}{PL_{SR_i}(d_{SR_i})}}\xi_{T_f}(h_{SR_i}) + \underbrace{\sum_{j=0}^{N_f-1}\bar{n}_{SR_i}(j)}_{\hat{n}_{SR_i}}. \tag{5}$$

With $\{b_{R_i}\}_{i=1}^m$, distributed space-time block coding (STBC) is applied at relays to achieve spatial diversity gain [14]. Let $\mathbf{B}$ be the STBC matrix with dimension $m \times N_f'$, where N_f' is the block length. Examples of the STBC matrix are shown in Table 2. In this paper, we assume that $N_f = QN_f'$ and Q is an integer. Thus, N_f frames are divided into Q frame blocks and the transmitted signal vector from relays in the second hop can be modeled as

$$\mathbf{t}_R(t) = \sqrt{P_{max}}\sum_{q=1}^{Q}\hat{\mathbf{b}}_R\hat{\mathbf{K}}_R\hat{\mathbf{W}}_R\mathbf{B}\boldsymbol{\omega}(t-N_fT_f, q), \tag{6}$$

where $\mathbf{t}_R(t) = [t_{R_1}(t), t_{R_2}(t), \ldots, t_{R_m}(t)]^T$ and the element $t_{R_i}(t)$ represents the transmitted signal at relay i. P_{max} is the maximum transmit power at each relay, which is constrained by FCC regulations. $\hat{\mathbf{b}}_R \triangleq \text{diag}\{b_{R_1}, \ldots, b_{R_m}\}$. $\hat{\mathbf{K}}_R \triangleq \text{diag}\{|b_{R_1}|^{-1}, \ldots, |b_{R_m}|^{-1}\}$ and $|x|$ represents the absolute value of x. $|b_{R_i}| = (\frac{N_f^2 P_s \xi_{T_f}^2(h_{SR_i})}{PL_{SR_i}(d_{SR_i})} + N_f\xi_{T_f}(h_{SR_i})\sigma^2)^{\frac{1}{2}}$. $\hat{\mathbf{W}}_R \triangleq \text{diag}\{w_1, \ldots, w_m\}$ is the diagonal matrix of the relay power allocation weights and $0 \le w_i \le 1$. Clearly, the transmit power of relay i is $w_i^2 P_{max}$. We define $\boldsymbol{\omega}(t,q) \triangleq [\omega(t-N_f'(q-1)T_f), \omega(t-N_f'(q-1)T_f-T_f), \ldots, \omega(t-N_f'(q-1)T_f-(N_f'-1)T_f)]^T$ is the waveform vector with length N_f'.

After passing through channels from relays to D, the received signal at D can be represented by

$$\begin{aligned} r_D(t) =& \sqrt{P_{max}}\sum_{q=1}^{Q}\sum_{i=1}^{m}\frac{\mathbf{e}_i^T\hat{\mathbf{b}}_R\hat{\mathbf{K}}_R\hat{\mathbf{W}}_R\mathbf{B}\mathbf{g}_{R_iD}(t-N_fT_f, q)}{\sqrt{PL_{R_iD}(d_{R_iD})}} \\ &+ n_D(t), \end{aligned} \tag{7}$$

where $\mathbf{e}_i$ is the ith column of the identity matrix. $\mathbf{g}_{R_iD}(t,q) \triangleq [g_{R_iD}(t-N_f'(q-1)T_f), g_{R_iD}(t-N_f'(q-1)T_f-T_f), \ldots, g_{R_iD}(t-N_f'(q-1)T_f-(N_f'-1)T_f)]^T$ and $g_{R_iD}(t) = \omega(t) * h_{R_iD}(t)$. $n_D(t)$ is the AWGN with zero mean and variance σ^2.

At D, a Rake receiver with L_r fingers is employed and the delayed reference waveforms $\{\omega(t-\tau(l_r))\}_{l_r=0}^{L_r-1}$ are used. After combining the Rake outputs over N_f' frames in each

Table 2: Examples of STBC matrix B for relays

m	N_f'	$\mathbf{B}$
2	2	$\begin{pmatrix} 1 & -1 \\ 1 & 1 \end{pmatrix}$
3	4	$\begin{pmatrix} 1 & -1 & -1 & -1 \\ 1 & 1 & 1 & -1 \\ 1 & -1 & 1 & 1 \end{pmatrix}$
4	4	$\begin{pmatrix} 1 & -1 & -1 & -1 \\ 1 & 1 & 1 & -1 \\ 1 & -1 & 1 & 1 \\ 1 & 1 & -1 & 1 \end{pmatrix}$

frame block, the output per frame block can be written as

$$\begin{aligned} z_D &= \sqrt{P_{max}} \sum_{l_r=0}^{L_r-1} \boldsymbol{\beta}_{RD}^T(l_r)\mathbf{B}\mathbf{B}^T\hat{\mathbf{K}}_R\hat{\mathbf{W}}_R\hat{\mathbf{PL}}_{RD}\mathbf{b}_R + \bar{n}_D(t) \\ &= N_f'\sqrt{P_{max}}\boldsymbol{\xi}_{RD}^T\hat{\mathbf{K}}_R\hat{\mathbf{W}}_R\hat{\mathbf{PL}}_{RD}\mathbf{b}_R + \bar{n}_D \end{aligned} \tag{8}$$

where $l_r \in [0, L_r - 1]$. $\mathbf{b}_R = [b_{R_1}, \ldots, b_{R_m}]^T$. $\boldsymbol{\beta}_{RD}(l_r) \triangleq [\beta^2_{R_1D}(l_r), \ldots, \beta^2_{R_mD}(l_r)]^T$ and $\beta_{R_iD}(l_r) = \int_0^{T_f} g_{R_iD}\omega(t - \tau(l_r))dt$. $\hat{\mathbf{PL}}_{RD} \triangleq \text{diag}\{PL^{-\frac{1}{2}}_{R_1D}(d_{R_1D}), \ldots, PL^{-\frac{1}{2}}_{R_mD}(d_{R_mD})\}$. $\boldsymbol{\xi}_{RD} \triangleq [\xi_{R_1D}, \ldots, \xi_{R_mD}]^T$ and $\xi_{R_iD} = \sum_{l_r=0}^{L_r-1}\beta^2_{R_iD}(l_r)$. Notice that ξ_{R_iD} represents the captured multipath energy from link R_i to D. $\bar{n}_D$ is the AWGN with zero mean and variance $N_f'\sum_{i=1}^m \xi_{R_iD}\sigma^2$.

Summing up all outputs over Q frame blocks and substituting (5) into (8), the decision variable for b can be given by

$$\begin{aligned} \hat{z} &= N_f\sqrt{P_{max}}\boldsymbol{\xi}_{RD}^T\hat{\mathbf{K}}_R\hat{\mathbf{W}}_R\hat{\mathbf{PL}}_{RD}\mathbf{b}_R + \hat{n}_D \\ &= bN_f^2\sqrt{P_{max}P_s}\boldsymbol{\xi}_{RD}^T\hat{\mathbf{K}}_R\hat{\mathbf{W}}_R\hat{\mathbf{PL}}_{RD}\hat{\mathbf{PL}}_{SR}\boldsymbol{\xi}_{SR} \\ &\quad + N_f\sqrt{P_{max}}\boldsymbol{\xi}_{RD}^T\hat{\mathbf{K}}_R\hat{\mathbf{W}}_R\hat{\mathbf{PL}}_{RD}\hat{\mathbf{n}}_{SR} + \hat{n}_D, \end{aligned} \tag{9}$$

where $\hat{\mathbf{PL}}_{SR} \triangleq \text{diag}\{PL^{-\frac{1}{2}}_{SR_1}(d_{SR_1}), \ldots, PL^{-\frac{1}{2}}_{SR_m}(d_{SR_m})\}$ and $\boldsymbol{\xi}_{SR} \triangleq [\xi_{T_f}(h_{SR_1}), \ldots, \xi_{T_f}(h_{SR_m})]^T$. $\hat{\mathbf{n}}_{SR} \triangleq [\hat{n}_{SR_1}, \ldots, \hat{n}_{SR_m}]^T$. $\hat{n}_D$ is the AWGN with zero mean and variance $N_f\sum_{i=1}^m \xi_{R_iD}\sigma^2$.

In (9), we identify three components

$$\hat{z}_s = bN_f^2\sqrt{P_{max}P_s}\boldsymbol{\xi}_{RD}^T\hat{\mathbf{K}}_R\hat{\mathbf{W}}_R\hat{\mathbf{PL}}_{RD}\hat{\mathbf{PL}}_{SR}\boldsymbol{\xi}_{SR}, \tag{10}$$

$$\hat{z}_{n_{SR}} = N_f\sqrt{P_{max}}\boldsymbol{\xi}_{RD}^T\hat{\mathbf{K}}_R\hat{\mathbf{W}}_R\hat{\mathbf{PL}}_{RD}\hat{\mathbf{n}}_{SR}, \tag{11}$$

and

$$\hat{z}_{n_{RD}} = \hat{n}_D, \tag{12}$$

as the useful signal, noise from the first hop, and noise from the second hop, respectively.

Obviously, the SE optimization based beamforming design is to find the optimal $\mathbf{w}_R = [w_1, \ldots, w_m]^T$ to maximize the received SE, which is equivalent to the optimal relay power allocation. In the next section, the optimal relay power allocation in (9) is investigated.

4. OPTIMAL POWER ALLOCATION

In this section, we analyze the optimal relay power allocation at relays. Since SE is a monotonically increasing function of the received signal to noise ratio (SNR), the received SNR is optimized accordingly.

Based on (9)-(12), the received SNR SNR_D can be expressed as

$$\text{SNR}_D(\mathbf{w}_R) = \frac{\text{E}\{|\hat{z}_s|^2\}}{\text{E}\{|\hat{z}_{n_{SR}}|^2\} + \text{E}\{|\hat{z}_{n_{RD}}|^2\}}. \tag{13}$$

Using (10), we have

$$\text{E}\{|\hat{z}_s|^2\} = \mathbf{w}_R^T\mathbf{O}_s\mathbf{w}_R, \tag{14}$$

where $\mathbf{O}_s = N_f^4P_{max}P_s\mathbf{V}\mathbf{V}^T$ and $\mathbf{V} = \hat{\boldsymbol{\xi}}_{RD}\hat{\mathbf{K}}_R\hat{\mathbf{PL}}_{RD}\hat{\mathbf{PL}}_{SR}\boldsymbol{\xi}_{SR}$. $\hat{\boldsymbol{\xi}}_{RD} \triangleq \text{diag}\{\xi_{R_1D}, \ldots, \xi_{R_mD}\}$.

Using (11), we have

$$\text{E}\{|\hat{z}_{n_{SR}}|^2\} = \mathbf{w}_R^T\mathbf{O}_n\mathbf{w}_R, \tag{15}$$

where $\mathbf{O}_n = N_f^3P_{max}\sigma^2\hat{\boldsymbol{\xi}}^2_{RD}\hat{\mathbf{K}}^2_R\hat{\mathbf{PL}}^2_{RD}\hat{\boldsymbol{\xi}}_{SR}$ and $\hat{\boldsymbol{\xi}}_{SR} \triangleq \text{diag}\{\xi_{T_f}(h_{SR_1}), \ldots, \xi_{T_f}(h_{SR_m})\}$.

From (12), we obtain

$$\text{E}\{|\hat{z}_{n_{RD}}|^2\} = N_f\sum_{i=1}^m \xi_{R_iD}\sigma^2. \tag{16}$$

Using (13)-(16), the distributed beamforming problem can be written as

$$\begin{aligned} &\underset{\mathbf{w}_R}{\text{maximize}} && \frac{\mathbf{w}_R^T\mathbf{O}_s\mathbf{w}_R}{\mathbf{w}_R^T\mathbf{O}_n\mathbf{w}_R + N_f\sum_{i=1}^m \xi_{R_iD}\sigma^2} \\ &\text{subject to} && \mathbf{0}_m \preceq \mathbf{w}_R \preceq \mathbf{I}_m, \end{aligned} \tag{17}$$

where $\mathbf{0}_m$ is a m-dimensional vector with all zero entries and $\mathbf{I}_m$ is a m-dimensional vector with all one entries. With two m-dimensional vectors $\mathbf{a}$ and $\mathbf{c}$, $\mathbf{a} \preceq \mathbf{c}$ means $a_i \leq c_i$ for all $i \in [1, m]$.

With an auxiliary variable δ[15], (17) is equivalent to

$$\begin{aligned} &\underset{\mathbf{w}_R,\delta}{\text{maximize}} && \delta \\ &\text{subject to} && \frac{\mathbf{w}_R^T\mathbf{O}_s\mathbf{w}_R}{\mathbf{w}_R^T\mathbf{O}_n\mathbf{w}_R + N_f\sum_{i=1}^m \xi_{R_iD}\sigma^2} \geq \delta^2 \\ &&& \mathbf{0}_m \preceq \mathbf{w}_R \preceq \mathbf{I}_m. \end{aligned} \tag{18}$$

Introducing the following notations

$$\mathbf{U}^T\mathbf{U} \triangleq \begin{pmatrix} N_f\sum_{i=1}^m \xi_{R_iD}\sigma^2 & \mathbf{0}_m^T \\ \mathbf{0}_m & \mathbf{O}_n \end{pmatrix}, \tag{19}$$

$$\tilde{\mathbf{w}}_R \triangleq [1, \mathbf{w}_R^T]^T, \tag{20}$$

and

$$\tilde{\mathbf{V}} \triangleq [0, \mathbf{V}^T]^T, \tag{21}$$

(18) can be further written as

$$\begin{aligned} \underset{\tilde{\mathbf{w}}_R,\delta}{\text{maximize}} \quad & \delta \\ \text{subject to} \quad & N_f^2\sqrt{P_{max}P_s}\tilde{\mathbf{w}}_R^T\tilde{\mathbf{V}} \geq \delta\|\mathbf{U}\tilde{\mathbf{w}}_R\| \\ & \mathbf{0}_m \preceq \tilde{\mathbf{w}}_R \preceq \mathbf{I}_m \\ & \tilde{\mathbf{w}}_R^T\mathbf{e}_1 = 1. \end{aligned} \tag{22}$$

Since (22) is a quasiconvex problem, it can be reduced to the following feasibility problem

$$\begin{aligned} \text{find} \quad & \tilde{\mathbf{w}}_R \\ \text{subject to} \quad & N_f^2\sqrt{P_{max}P_s}\tilde{\mathbf{w}}_R^T\tilde{\mathbf{V}} \geq \delta\|\mathbf{U}\tilde{\mathbf{w}}_R\| \\ & \mathbf{0}_m \preceq \tilde{\mathbf{w}}_R \preceq \mathbf{I}_m \\ & \tilde{\mathbf{w}}_R^T\mathbf{e}_1 = 1. \end{aligned} \tag{23}$$

With (22) and (23), the bisection search method [15] can be used to find the optimal power allocation vector $\mathbf{w}_R^o$. Accordingly, the optimal SE can be given by $\frac{1}{2N_f}\log_2(1 + SNR_D(\mathbf{w}_R^o))$ [bits/s/Hz].

5. SIMULATION

To evaluate the SE of the proposed distributed beamforming scheme in UWB based IBANs, numerical results and examples are presented in this section. In simulations, T_w and T_f are chosen to be 0.7ns and 100ns, respectively. N_f is set to be 4. The noise power spectral density (PSD) is -174dBm/Hz and the system bandwidth is 1.4GHz. Since the average FCC PSD emission limit for UWB signals is -41.3dBm/MHz, the maximum average transmit power P_{ave} is -9.8dBm. With the duty cycle T_w/T_f, $P_{max} = P_{ave} * T_f/T_w \approx 12$dBm. For the transmit power of the implant node, we set $P_s \leq 10$dBm considering the emission limit and safety inside the human body. According to the scale of the human body, d_{SD} and d_r are set to be 200mm and 50mm, respectively. At relays, we assume that $\xi_{T_f}(h_{SR_i}) \approx 1$ for all $i \in [1, m]$ without considering the ISI. At D, a selective Rake receiver is employed to combine the L_r strongest multipath components.

Fig. 2 shows the average SE versus P_s in a 2-relay UWB based IBANs. For this 2-relay case, we assume that the coordinates of the two relays are set to be $\{(90, 20)\}$ and $\{(90, -20)\}$, respectively. Performance of the proposed distributed beamforming scheme is compared to those of the equal power allocation (EPA) scheme (every relay uses its maximum power), best-relay selection (S-AF) scheme (the relay with the highest SNR is selected), and direct transmission. We can see that the proposed distributed beamforming scheme outperforms all the other schemes. With perfect channel information at relays, it is about 5dB better than the OPA scheme which needs no channel information about the second hop at relays. Compared to direct transmission, we can see that the proposed distributed beamforming scheme can provide more than 16dB performance improvement and this improvement mainly results from the fact that the path loss of the"in-body to on-body" link is much stronger than that of the "on-body to on-body" link. From the perspective of power consumption, the transmit power at S by using distributed beamforming scheme is much less (more than 28dB)

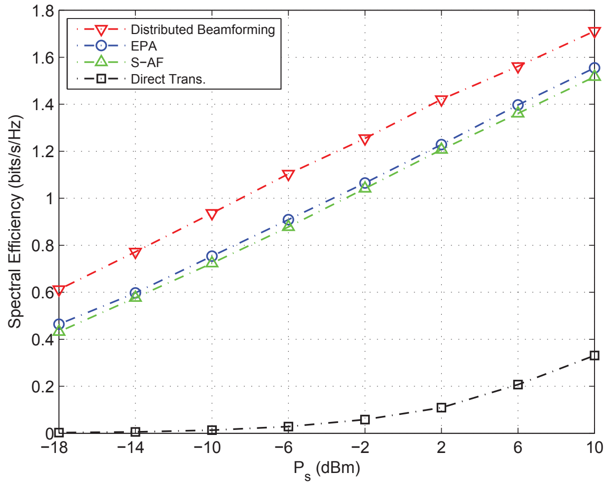

Figure 2: Average SE versus P_s with $L_r = 4$ in a 2-relay network.

compared to that by direct transmission when the same SE is achieved. This evidence indicates that the lifetime of the implant node can be prolonged considerably in distributed relay networks, which demonstrates the effectiveness of the proposed distributed beamforming scheme when applied to UWB based IBANs.

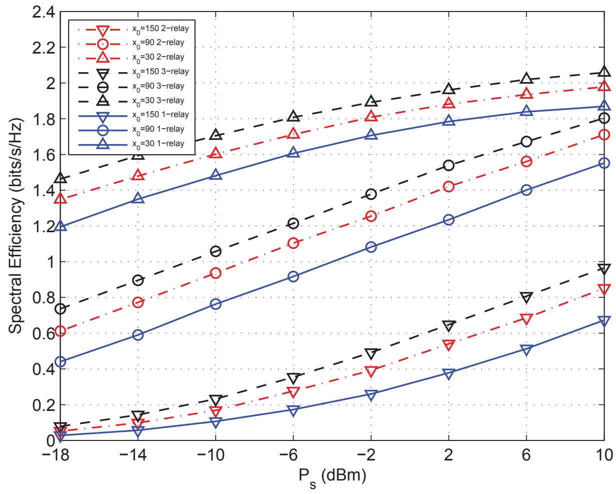

Figure 3: Average SE versus P_s with different numbers of relays and relay locations when $L_r = 4$.

Fig. 3 depicts the average SE versus P_s with different numbers of relays and relay locations. Specifically, three cases with $m = 1, 2,$ and 3 are considered, respectively. For the case $m = 1$, the coordinate of the single relay is set to be $\{(x_0, 0)\}$. For the case $m = 2$, the coordinates of the relays are set to be $\{(x_0, 20)\}$ and $\{(x_0, -20)\}$, respectively. For the case $m = 3$, the coordinates of the relays are set to be $\{(x_0, 20)\}$, $\{(x_0, 0)\}$, and $\{(x_0, -20)\}$, respectively. For all the cases, x_0 is set to be $30, 90,$ and 150, respectively, where $x_0 = 30$ represents that relays are close to P, $x_0 = 90$

represents that relays are located near the middle of P and D, and $x_0 = 150$ represents that relays are close to D. As shown in this figure, the SE performance improves when the number of relays is increased. This improvement benefits from the spatial diversity offered by multiple-relay channels. Thus, given a targeted SE, employing more relays can improve the power efficiency of the implant node. On the other hand, it is shown that the relay location plays an important role for the distributed relay IBANs. With a given P_s, the SE performance of the proposed distributed beamforming scheme is sensitive to the relay location and the SE is the highest when relays are at $x_0 = 30$ among all three locations. Based on these observations, it is concluded that the relay location is an influential parameter in UWB based IBANs. Choosing relays with proper locations can enhance the system performance effectively.

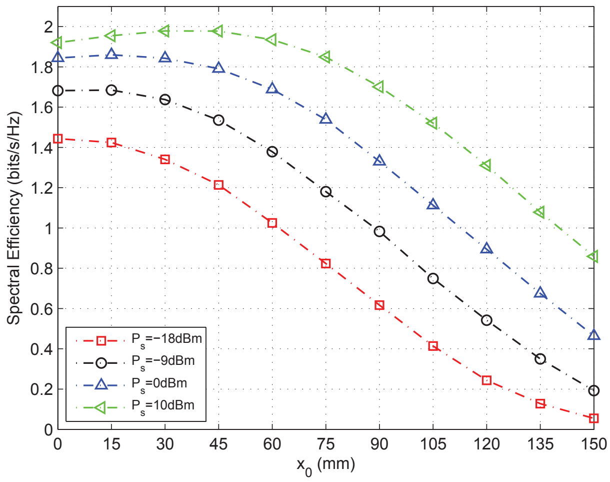

Figure 4: Average SE versus x_0 with different P_s in a 2-relay network.

To further investigate the impact of relay location, the average SE versus x_0 with different P_s in a 2-relay UWB based IBANs is illustrated in Fig. 4. The coordinates of the two relays are set to be $\{(x_0, 20)\}$ and $\{(x_0, -20)\}$, respectively. From this figure, we notice that the optimal x_0 exists with a fixed P_s and the optimal x_0 varies with P_s. When the battery power of S is very limited and $P_s = -18$dBm, employing the relays at P can achieve the utmost SE. As P_s becomes larger, the optimal x_0 increases and choosing the relays close to P is the best option.

Fig. 5 presents the average SE versus P_s with different L_r in a 2-relay network, where the locations of the two relays are set to be $\{(30, 20)\}$ and $\{(30, -20)\}$, respectively. Obviously, employing more Rake fingers can achieve better SE performance because more multipath energy can be captured. From the power consumption viewpoint, the lifetime of the implant node can be prolonged at the cost of deploying more Rake fingers at D.

In conclusion, the proposed distributed beamforming scheme can be applied to UWB based IBANs effectively, which is superior to other transmission schemes. In distributed relay IBANs, the lifetime of the implant node can be prolonged at the cost of deploying more relays and more Rake fingers at D with a targeted SE. Moreover, the relay location has a significant impact on the system performance and choosing relays close to P can achieve a better system performance compared to that with other relay locations.

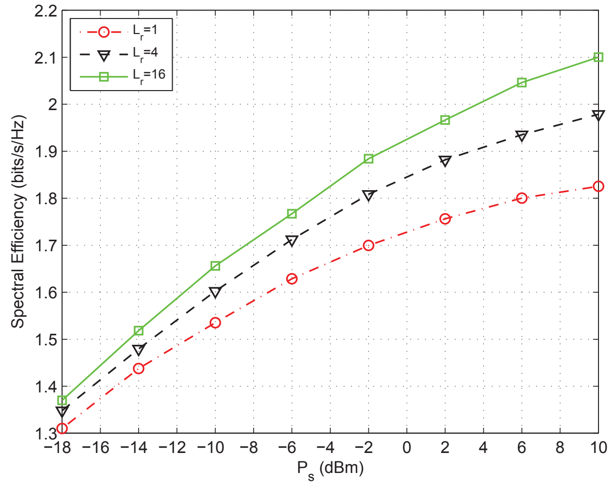

Figure 5: Average SE versus P_s with different L_r in a 2-relay network.

6. CONCLUSIONS

In this paper, we investigate the SE optimization problem with distributed beamforming in UWB based IBANs. The proposed network beamforming scheme is equivalent to solving a distributed power allocation problem, where each relay properly adjusts its own power such that the system SE can be maximized. Numerical examples demonstrate the effectiveness of the proposed distributed beamforming scheme when applied to UWB based IBANs. We further show that the relay location is an influential parameter in UWB based IBANs. The system performance with different relay locations may have a notable difference. Thus, the effect of relay location cannot be ignored. Moreover, from the power efficiency point of view, the proposed beamforming scheme is shown to be a promising way to enhance the power efficiency of the implant node and prolong its lifetime.

7. REFERENCES

[1] Ieee standard for local and metropolitan area networks-part 15.6: Body area networks, 2012.

[2] M. Patel and J. Wang. Applications, challenges, and prospective in emerging body area networking technologies. IEEE Wireless Communications, 17(1):80–88, 2010.

[3] A. Nosratinia, T. Hunter, and A. Hedayat. Cooperative communication in wireless networks. IEEE Communications Magzine, 42:68–73, 2004.

[4] Y. Zhao, R. Adve, and T. J. Lim. Improving amplify-and-forward relay networks: optimal power allocation versus selection. IEEE Transactions on Wireless Communications, 6:3114–3122, 2007.

[5] Y. Jing and H. Jafarkhani. Network beamforming

using relays with perfect channel information. IEEE Transactions on information theory, 55(6):2499–2517, 2009.

[6] V. Havary-Nassab, S. Shahbazpanahi, A. Grami, and Z.-Q. Luo. Distributed beamforming for relay networks based on second-order statistics of the channel state information. IEEE Transactions on Signal Processing, 56:4306–4316, 2008.

[7] H. Chen, A. B. Gershman, and S. Shahbazpanahi. Filter-and-forward distributed beamforming in relay networks with frequency selective fading. IEEE Transactions on Signal Processing, 58(3):1251–1261, 2010.

[8] S. Zhu and K. K. Leung. Cooperative orthogonal mimo-relaying for uwb ad-hoc networks. In Proc. IEEE Globecom, pages 5175–5179, 2007.

[9] K. Maichalernnukul, T. Kaiser, and F. Zheng. Performance investigation of a uwb relay system using multiple relays with multiple antennas in ieee 802.15.3a channel. In Proc. IEEE VTC, pages 1–6, 2009.

[10] S. Zhu, K. K. Leung, and A. G. Constantinides. Distributed cooperative data relaying for diversity in impulse-based uwb ad-hoc networks. IEEE Transactions on Wireless Communications, 8(8):4037–4047, 2009.

[11] M. Mondelli, Q. Zhou, X. Ma, and V. Lottici. A cooperative approach for amplify-and-forward differential transmitted reference ir-uwb relay systems. In Proc. IEEE ICASSP, pages 2905–2908, 2012.

[12] K. Y. Yazdandoost and K. Sayrafian-Pour. Channel model for body area network (ban). Technical Report IEEE802.15-08-0780-05-0006, IEEE P802.15 Working Group for Wireless Personal Area Networks (WPANs), 2009.

[13] A. Khaleghi, R. Chávez-Santiago, and I. Balasingham. Ultra-wideband statistical propagation channel model for implant sensors in the human chest. IET Microwaves, Antennas and Propagation, 5(15):1805–1812, 2011.

[14] L. Yang and G. B. Giannakis. Analog space-time coding for multiantenna ultra-wideband transmissions. IEEE Transactions on Communications, 52:507–517, 2004.

[15] S. Boyd and L. Vandenberghe. Convex Optimization. Cambridge University Press, 2004.